

**Assessing CSF ctDNA to improve diagnostic accuracy and therapeutic monitoring in  
breast cancer leptomeningeal metastasis**

Amanda Fitzpatrick<sup>1</sup>, Marjan Iravani<sup>1</sup>, Adam Mills<sup>1</sup>, Lucy Childs<sup>2</sup>, Thanussuyah Alaguthurai<sup>3</sup>,  
Angela Clifford<sup>3</sup>, Isaac Garcia-Murillas<sup>1</sup>, Steven van Laere<sup>4</sup>, Luc Dirix<sup>5</sup>, Mark Harries<sup>6</sup>,  
Alicia Okines<sup>7</sup>, Nicholas C. Turner<sup>1,7</sup>, Syed Haider<sup>1</sup>, Andrew N. J. Tutt<sup>1,3</sup>, Clare M. Isacke<sup>1,\*</sup>

<sup>1</sup>The Breast Cancer Now Toby Robins Research Centre, The Institute of Cancer Research;  
London, UK

<sup>2</sup>Department of Clinical Radiology, Guy's & St Thomas' NHS Foundation Trust; London, UK

<sup>3</sup>Breast Cancer Now Research Unit, Guy's Hospital, King's College London; London, UK

<sup>4</sup>Translational Cancer Research Unit (TCRU), GZA Ziekenhuizen; Antwerp, Belgium

<sup>5</sup>Medical Oncology, GZA Hospital Sint-Augustinus; Antwerp, Belgium

<sup>6</sup>Department of Medical Oncology, Guy's & St Thomas' NHS Foundation Trust; London, UK

<sup>7</sup>The Royal Marsden NHS Foundation Trust; London, UK

**Running title:** ctDNA detection in breast cancer leptomeningeal metastasis

**\*Corresponding Author:** Professor Clare M. Isacke, The Breast Cancer Now Toby Robins  
Research Centre, The Institute of Cancer Research, 237 Fulham Road, London SW3 6JB,  
UK. Telephone +44 20 7153 5510, Email clare.isacke@icr.ac.uk

**Conflicts of Interest**

All authors have declared no conflicts of interest for this work

## **Translational Relevance**

There is an urgent need for progress in the management of breast cancer leptomeningeal metastasis (BCLM). Current diagnostics are hampered by impaired sensitivity, delaying diagnosis and treatment initiation. Further, during BCLM therapy there are no quantitative response markers to guide clinical decision making. This proof-of-concept study explored the use of ulpWGS, a methodology requiring no upfront knowledge of tumor mutations, to detect ctDNA in cerebrospinal fluid (CSF) in BCLM. ctDNA was detectable in all BCLM+ patients by ulpWGS, despite frequent negative CSF cytology. Importantly, CSF ctDNA was not detected in BCLM-free patients, supporting the potential for ulpWGS as a tool to refute diagnosis. In addition, CSF ctDNA reduction, measured by ulpWGS, was associated with improved survival on intrathecal BCLM treatment. This study highlights the potential of ulpWGS-assessed CSF ctDNA fraction to improve BCLM care through timely diagnosis and adaptation of therapy, and warrants larger prospective studies to test clinical validity.

## **Abstract**

**Purpose:** Cerebrospinal fluid (CSF) cytology is the gold standard diagnostic test for breast cancer leptomeningeal metastasis (BCLM), but has impaired sensitivity, often necessitating repeated lumbar puncture to confirm or refute diagnosis. Further, there is no quantitative response tool to assess response or progression during BCLM treatment.

**Experimental design:** Facing the challenge of working with small volume samples and the lack of common recurrent mutations in breast cancers, cell-free DNA was extracted from CSF and plasma of patients undergoing investigation for BCLM ( $n=30$ ). ctDNA fraction was assessed by ultra-low pass whole genome sequencing (ulpWGS), which does not require prior tumor sequencing.

**Results:** In this proof-of-concept study ctDNA was detected (fraction  $\geq 0.10$ ) in CSF of all 24 BCLM+ patients (median ctDNA fraction 0.57), regardless of negative cytology or borderline MRI imaging, whereas CSF ctDNA was not detected in the 6 BCLM- patients (median ctDNA fraction 0.03,  $P<0.0001$ ). Plasma ctDNA was only detected in patients with extracranial disease progression or who had previously received whole brain radiotherapy. ctDNA fraction was highly concordant with mutant allele fraction measured by tumor mutation-specific ddPCR assays ( $r=0.852$ ,  $P<0.0001$ ). During intrathecal treatment, serial monitoring ( $n=12$  patients) showed that suppression of CSF ctDNA fraction was associated with longer BCLM survival ( $P=0.034$ ) and rising ctDNA fraction was detectable up to 12 weeks before clinical progression.

**Conclusion:** Measuring ctDNA fraction by ulpWGS is a quantitative marker demonstrating potential for timely and accurate BCLM diagnosis and therapy response monitoring, with the ultimate aim to improve management of this poor prognosis patient group.

## **Introduction**

Metastasis to the leptomeninges (LM) occurs in 5-10% of patients with metastatic breast cancer (1) and, despite advances in breast cancer treatments, the median survival after the diagnosis of BCLM remains only 3-4 months (2-4). Clinical case series have shown the strongest negative prognostic factor in LM is poor performance status (4) therefore diagnosing earlier with prompt initiation of LM-directed therapy, before significant decline in neurological function, may lead to improved survival. Currently, rapid and robust diagnosis remains a significant challenge in LM. Diagnosis has traditionally centred on the cytological assessment of cerebrospinal fluid (CSF) obtained by lumbar puncture, which has 100% specificity upon the finding of malignant cells in CSF (5), however is hampered by a high false negative rate, with sensitivity of just 45-67% at the first lumbar puncture (6-8). Consequently, around one third of patients undergo repeated lumbar puncture (5), with sensitivity rising to 80-89% (6,7,9) albeit at the cost of not only additional morbidity but delays in diagnosis and initiation of therapy.

Although improvements in LM diagnosis have been achieved with contrast-enhanced high field magnetic resonance imaging (MRI), it remains an imperfect diagnostic tool. Sensitivity of MRI for LM diagnosis is 76-86% (5,8,10,11) with specificity of 77% (5). Furthermore, neuroimaging findings in LM (12) can be subjective with difficulty in standardizing findings between radiologists and heterogeneity in the imaging protocols used (13).

The recent EANO-ESMO Clinical Practice Guidelines for diagnosis, treatment and follow-up of patients with LM from solid tumors (14) continue to recommend CSF cytology alongside MRI imaging as part of the diagnostic work up, and recommend that repeat lumbar puncture should be performed upon initial negative or equivocal CSF studies. Further, the LM treatment algorithm recommends a therapeutic approach which includes intrathecal chemotherapy when CSF cytology is positive. Intrathecal chemotherapy remains the standard of care treatment in LM despite a lack of randomised trials showing benefit (15).

More recently, BCLM patients with HER2+ breast cancer have been successfully treated with intrathecal trastuzumab (16,17). These invasive therapies require close monitoring and judicious response assessment to ensure continued benefit, however there are no LM quantitative biomarkers and MRI findings are not easily measurable. Intrathecal treatment protocols recommend reduction in dosing intensity when CSF cytology 'clears' however given the high false negative cytology rate, this is not always a reliable marker of response.

CSF, similar to plasma and other body fluids, contains circulating cell-free DNA (cfDNA) and in the presence of malignancy a fraction is tumor-derived (ctDNA). In a study of 12 patients with primary brain tumors or brain metastases, ctDNA was demonstrated to be more abundant in CSF than plasma when tumor involvement was predominant in the central nervous system (CNS) (18). Studies determining presence of CSF ctDNA have mostly employed droplet digital PCR (ddPCR), detecting highly prevalent hotspot mutation, such as BRAF<sup>V600E</sup> in melanoma (19) or EGFR<sup>T790M</sup> in lung adenocarcinoma (20-22). However, in breast cancer there are few hotspot mutations, and broad sequencing of the matched primary tumor is required for the identification of patient-specific somatic mutations (23). This process can be both time-consuming and costly, making it a suboptimal approach when a rapid diagnosis of LM is required.

In this proof-of-concept study we demonstrate the potential utility of using ultra-low pass whole genome sequencing (ulpWGS), a relatively low-cost and rapid tool which does not require prior knowledge of the tumor mutational landscape, to detect ctDNA in CSF of patients in BCLM for diagnosis and monitoring of response to intrathecal therapy.

## **Methods**

### **Patients, sample collection and processing**

CSF was prospectively collected by lumbar or ventricular route (Ommaya reservoir or ventriculoperitoneal shunt), from breast cancer patients at initial evaluation for known or suspected BCLM ( $n=30$ ). In 27 patients, baseline blood samples were collected concurrently. Written informed consent was obtained from all individuals in accordance with the Declaration of Helsinki under the following research ethics committee approved studies (REC ID 13/LO/1248, South East London Cancer Research Network, UK, and REC ID 14/LO/0292, Royal Marsden NHS Foundation Trust, UK, and local ethics committee GZA Hospital Sint-Augustinus, Antwerp).

Baseline neuroaxis MRI imaging was reviewed by an independent consultant neuroradiologist to evaluate cases where initial reporting was either borderline or negative for BCLM. CSF cytology reports were categorized as equivocal if findings were suspicious but not confirmatory for the presence of malignant cells, and otherwise classified as positive or negative.

Serial CSF and blood samples were collected immediately prior to administration of intrathecal therapy in 12 patients. In patients who did not undergo intrathecal therapy no further samples were obtained.

Following defined Standard Operating Procedures, samples were handled as follows: CSF samples were collected in standard universal containers and transported on wet ice to the laboratory, for centrifugation within 1 hour of collection at 300g for 10 minutes. CSF cell-free supernatant was stored at  $-80^{\circ}\text{C}$ . Peripheral blood was collected in EDTA tubes and centrifuged within 4 hours, at 1600g for 20 minutes to obtain plasma and buffy coat, both were stored at  $-80^{\circ}\text{C}$  until extraction. CSF total protein levels were recorded from hospital records. For cfDNA extraction, CSF supernatant and plasma were thawed at  $4^{\circ}\text{C}$ , extraction

performed using the Qiagen Circulating Nucleic Acid kit following the manufacturer's instructions with the following optimization: elution buffer volume of 50  $\mu$ L remained on the column for 20 minutes at room temperature prior to final centrifugation. The extracted cfDNA was quantified by Qubit Fluorometer 2.0 using the Qubit dsDNA High Sensitivity Assay Kit, and thereafter stored in DNA LoBind® tubes at -20°C. Germline DNA was extracted from buffy coat using the Qiagen DNeasy Blood and Tissue Kit. Genomic DNA (gDNA) was obtained from archival primary tumor blocks using the QIAamp DNA AllPrep FFPE Kit, following macrodissection of Nuclear Fast Red-stained tissue sections to obtain maximum tumor cellularity. DNA was quantified using a Qubit Fluorometer 2.0 using the Qubit dsDNA Broad Range Assay Kit.

#### **Ultra-low pass whole genome sequencing (ulpWGS) of CSF and plasma cfDNA**

0.5-20 ng CSF/plasma cfDNA or buffy coat gDNA underwent ulpWGS library preparation using the NEBNext Ultra II DNA Library Prep Kit for Illumina, with 6-15 cycles of PCR enrichment. Samples were indexed using NEBNext Multiplex Oligos for Illumina. Resultant libraries were pooled and sequenced on a NovaSeq 6000, acquiring 2 x 100 bp reads. No samples failed library preparation or sequencing, and depth of coverage across all samples was 0.26X (median). ulpWGS FASTQ files were aligned against the human assembly build GRCh38 using (BWA) v0.7.17, duplicate reads were removed with Picard v2.23.8 and mean coverage of aligned reads were derived from the deduplicated BAM file using the CollectWgsMetrics (Picard v2.23.8) tool. Using ichorCNA (24) estimates of tumor purity and copy-number aberrations were generated. HMMcopy readCounter v1.1.0 was used to divide the genome into non-overlapping bins of either 50 kb or 1 Mb. Centromeres were filtered based on chromosome gap coordinates obtained from UCSC for GRCh38. Aligned reads from the overlap within each window were normalized to correct for GC-content and mappability biases. The  $\log_2$  ratio copy-number profiles were generated for each window relative to a panel of matched germline DNA that were sequenced concurrently. The

ichorCNA parameters were set as follows: *n* (normal fraction) values of 0.6, 0.7, 0.8 and 0.9; ploidy initial values of 2 or 3; and subclone fraction estimation not enabled.

### **ddPCR of CSF and plasma cfDNA**

To identify patient-specific somatic variants for CSF and plasma cfDNA ddPCR analysis, primary tumor and matched germline DNA were subjected to hybridization capture to either Human All Exome V6 panel for whole exome sequencing (WES) or a targeted custom-designed capture panel. For WES, library preparation was performed using the SureSelect XT Library preparation kit. Post-capture libraries were run on the NovaSeq 6000 acquiring 2 x 100 bp paired-end reads. Median coverage across all samples was 223X. Reads were aligned against GRCh38 using Burrows-Wheeler Aligner (BWA) v0.7.15, deduplication by Picard v2.0.1. SNV and indel variant calling on paired tumor/normal was performed with Mutect2 (25), and all variants annotated by ANNOVAR (2016-02-01 version) (26). For target panel sequencing, DNA samples were sequenced using a targeted, custom-designed capture panel (RMH200 v1.3.1 panel) consisting of 233 cancer related genes (27). NGS libraries were prepared using the KAPA HyperPlus Kit and Integrated DNA Technologies UDI 8 bp adapters, followed by target enrichment by hybridization to a custom DNA bait library (Nimblegen), and underwent 2 x 100 bp paired-end sequencing on NovaSeq 6000. Mean coverage across all samples was 280X. Analysis was performed using an in-house developed pipeline Molecular Diagnostic Information Management System version 3.0 (MDIMSV3) using the following bioinformatic software and versions: demultiplexing by bcl2fastq 2.17.1.14 to isolate reads for each sample, read alignment against GRCh37 by BWA v0.7.15, SNVs and indel calling by Mutect2 from the GATK 3.5.0 suite. Variants were annotated by Personal Cancer Genome Reporter v.0.6 (PCGR). In cases where primary tumor was not obtainable, sequencing was performed on plasma cfDNA (*n*=3), metastasis tissue (*n*=1) or CSF tumor cells (*n*=1).

Patient-specific candidate somatic driver mutations for ddPCR assay development were identified from targeted panel/WES of matched tumor and germline samples by the following criteria (a) cancer-associated hotspot variant (listed on <https://www.cancerhotspots.org>) and/or (b) variant with high allele frequency in a Cancer Gene Census gene (28). Candidate variants (Supplementary Table S2) were manually inspected on IGV prior to selection for ddPCR assay design. Custom ddPCR assays for *PIK3CA* p.H1047R/H1047L/E545K/E542K, *ERBB2* L755S, and *TP53* p.R196\*/R273H were designed in-house using primer3 software (<https://primer3.ut.ee/>). ddPCR assays for variants *HIF1A* p.A565G, *KNL1* p. I654V, *PIK3R1* p.450\_452del, *RB1* p.S829X, *ANK1* p.A717T, *PIK3CA* p.G118D and *TP53* p.158fs/Q104\*/R158C/T253fs, were designed using Custom TaqMan® SNP Genotyping Design Tool (Thermo Fisher). Primers and probes, ordered from Thermo Fisher and detailed in Supplementary Table S3, were used at a final concentration of 900 nM and 250 nM respectively. Commercially available assays for *AKT1* p.E17K and *ATM* p.R337H were purchased from Bio-Rad (Supplementary Table S4). ddPCR was performed as previously described (23). The exome sequenced tumor DNA was used to validate the mutation by ddPCR and determine the optimum cycling conditions prior to assaying the matched cfDNA samples. There was no minimum cfDNA input in the ddPCR assays, however where sufficient cfDNA was available, 10 ng of DNA was assayed. All runs included tumor DNA (positive control) and matched germline DNA (negative controls) and wells containing assay without DNA (non-target controls).

ddPCR analysis was performed on QuantaSoft Analysis Pro Software, version 1.7.4. Wells with total droplet count <10,000 were excluded, and a minimum of 2 mutant-FAM positive droplets per well was required to define the presence of tumor DNA. No sample was called positive for tumor content on the finding of only double (FAM and VIC) positive droplets, since these might represent false positives due to the introduction of polymerase driven errors during amplification.

Mutant allele fraction (MAF) was calculated as follows:

- ddPCR MAF = FAM (mutant) copies/ $\mu$ L / (FAM (mutant) copies/ $\mu$ L + VIC (wild-type) copies/ $\mu$ L)

To assess the number of mutant copies per mL, the number of mutant-FAM positive droplets was adjusted for the number of wells run for the sample, the total number of droplets generated, the median volume of a droplet (0.89 pL), and volume equivalent of CSF/plasma per run, using the following formula:

- ddPCR mutant copies per mL = (total number of droplets positive for FAM) x 20,000 x (number of wells run/volume of plasma equivalents) / (total number of droplets generated x 0.89)

When using ddPCR to determine MAF, the lower limit of detection (LoD) is determined by the total number of DNA molecules screened, i.e., the total DNA input. Since the DNA input varied per sample due to cfDNA yield, the minimum MAF detectable by ddPCR (LoD) for each sample was calculated using the following formula, and samples not achieving a ddPCR LoD of 0.10 were marked as failed:

- ddPCR limit of detection (LoD) = 3 / (haploid genome equivalents (FAM copies/ $\mu$ L + VIC copies/ $\mu$ L) x 20)

### **Statistical analysis**

All statistical analysis was performed with GraphPad Prism version 9.1.0 and R 3.6.2. All *P* values are two-sided and considered significant if *P* < 0.05. All comparisons between two groups were made using two-tailed, unpaired Student's *t*-test. If the analysis did not pass normality test (Shapiro–Wilk test) groups were analyzed by Mann Whitney *U*-test. If more than two groups were compared one-way ANOVA analysis was performed with post-hoc

Tukey's test for multiple comparison. Kaplan-Meier analysis using Log-rank (Mantel-Cox) test was used to assess BCLM overall survival.

## Results

### **Patient characteristics, central nervous system (CNS) imaging and CSF cytological diagnostics**

This study comprised 30 patients presenting with typical symptoms of CNS involvement (Table 1; Supplementary Table S1). 24/30 cases were diagnosed with confirmed BCLM by the treating oncology team, based on standard diagnostics and clinical assessments (BCLM+ group), and in 2 cases synchronous brain metastases (BCBM) were detected. The remaining 6 patients had suspected but non-confirmed BCLM, and at median 39.7 months follow-up had no evidence of BCLM (BCLM-). All 6 BCLM- patients were free of CNS metastasis at the time of CSF sampling, however 3/6 later developed BCBM at 9.5, 9.8 and 22.5 months, whilst remaining BCLM-free. In keeping with their known predilection for leptomeninges (8,29), lobular breast cancers were enriched in the BCLM+ group, comprising 46% (11/24) of cases. In line with this enrichment, the predominant immunohistological subtype was hormone receptor-positive (HR+) HER2-, comprising 67% (16/24), meanwhile HER2+ cases comprised 12.5% (3/24) of the BCLM+ cohort.

Standard diagnostics performed were: CSF cytology in 30/30 cases; cranial +/- spinal MRI in 29/30 cases. In 9/30 (30%) multiple diagnostic lumbar punctures were performed. In BCLM+ cases, CSF cytology was suspicious ( $n=2$ ) or negative ( $n=10$ ) in 12/24 (50%) on initial lumbar puncture. Final CSF cytology (following repeat) was positive in 17/24 (71%) of BCLM+ cases. All 6/6 BCLM- cases were negative on both initial and repeated cytology. In BCLM+ cases, MRI imaging was diagnostic in 20/23 (87%) with 3 scans remaining borderline following independent neuroradiologist review (Table 1). MRI imaging was negative in all BCLM- cases (1/6 had generalized dural thickening but no leptomeningeal enhancement).

### **CSF ctDNA fraction measured by ulpWGS correlates with BCLM diagnostic status**

CSF and plasma were collected at initial evaluation for BCLM ( $n=30$ ) and longitudinally during the course of intrathecal therapy in a subset of 12 BCLM+ patients (median 7.5 timepoints, range 2 – 11) (Fig. 1A). A median of 1.8 mL CSF (range 0.3 - 26.0 mL) and 3.8 mL plasma (range 1.0 - 12.0 mL) across all timepoints were obtained. CSF and plasma cfDNA were quantified (Fig. 1B) and fragment length assessed by capillary electrophoresis (Fig. S1A). cfDNA concentration was significantly lower in CSF vs. plasma (median CSF cfDNA 21.9 ng/mL, range 3.98 - 1363 ng/mL vs. plasma cfDNA 38.8 ng/mL, range 8.45 - 1773;  $P = 0.005$ ) (Fig. 1B) and coupled with the smaller volumes obtained, this resulted in lower total cfDNA yield from CSF samples, in line with previous reports (30,31).

To detect and quantify ctDNA fraction in CSF and plasma, we sought a tumor-agnostic approach requiring no prior sequencing of the patient's primary tumor, and a method suitable for low DNA input. To this aim, paired end, ulpWGS was performed on 141 cfDNA samples (95 CSF and 46 plasma) with sequencing libraries created from as little as 0.5 ng cfDNA (Fig. 1C). The equivalent sample volumes used for library preparation were median 0.54 mL CSF (range 0.05 - 3.96) and 0.72 mL plasma (range 0.01 - 2.40). ulpWGS provided an accurate assessment of ctDNA fragment length, revealing differing cfDNA fragmentation patterns, with the highest fraction of reads corresponding to a shorter fragment length of 152 bp in CSF vs. 166 bp in plasma ( $P < 0.0001$  by Mann-Whitney  $U$ -test) (Supplementary Fig. S1B).

ichorCNA (1 Mb bin size) was used to identify large-scale copy number aberrations and, through probabilistic modelling, to estimate tumor purity (ctDNA fraction) and ploidy (24). Representative examples in BCLM+ and BCLM- settings are shown in Fig. 1D. Further, performing ichorCNA analysis using a 50 kb bin size, focal gene amplifications were identified. Examples of *ERBB2* amplification in CSF are shown in Supplementary Fig. S2.

Overall, the ctDNA fraction in CSF was significantly higher in patients with a BCLM+ diagnosis ( $n=24$ , median 0.57, range 0.27 - 0.89) compared to BCLM- patients ( $n=6$ , median 0.03, range 0.00 - 0.08,  $P < 0.0001$ ) (Fig. 2A). Adalsteinsson *et al.* determined that ichorCNA analysis of ulpWGS data has a high degree of accuracy for ctDNA fraction  $\geq 0.10$  (24), consequently a cut-off of 0.10 was used in this study for ctDNA detection. CSF ctDNA fraction was  $\geq 0.10$  (detectable) in 100% of BCLM+ cases, and  $< 0.10$  in all BCLM- cases. Comparing CSF ctDNA fraction to standard BCLM diagnostics, ctDNA was above the detection level in all BCLM+ patients regardless of initial negative or suspicious CSF cytology (50% of BCLM+) (Fig 2A), and in those cases where MRI imaging was borderline (17% of BCLM+) (Fig. 2B). CSF collection site (lumbar vs. ventricular) did not impair CSF ctDNA detection (Supplementary Fig. S3A).

Of the 3/6 BCLM- cases who later developed BCBM, there was no difference in CSF ctDNA fraction compared to those who remained CNS-disease free (Fig. 2C).

These data suggest that determining the ctDNA fraction in CSF has greater diagnostic sensitivity in BCLM than CSF cytology or MRI, and correctly identifies patients who are BCLM-free. Furthermore, ulpWGS determination of tumor content was successful in all CSF samples and there was no requirement for further CSF sampling, contrary to the 33% of cases where repeated lumbar puncture was indicated for definitive CSF cytology. Of note, there was no correlation between extracted CSF cfDNA concentration (ng/mL) and CSF ctDNA fraction, indicating that cfDNA concentration alone cannot act as a surrogate for tumor fraction (Fig. 2D). Similarly, there was no correlation between the CSF volume collected and either cfDNA concentration or CSF ctDNA fraction (Supplementary Fig. S3B,C).

### **Plasma ctDNA fraction is determined by extracranial progression**

Consistent with previous reports (18), ctDNA fraction was significantly lower in plasma than CSF in BCLM+ cases (median ctDNA fraction in plasma 0.071 vs. in CSF 0.566,  $P < 0.0001$ ) with 12/22 plasma samples below ctDNA detection level. By contrast, in BCLM- cases there was no significant difference in ctDNA fraction between the 5 paired plasma and CSF samples (Fig. 2E). Plasma ctDNA was found to be detectable ( $\geq 0.10$  ctDNA fraction) only in those with progression of extracranial disease or who had previously received whole brain radiotherapy (Fig. 2F).

### **ulpWGS and ddPCR methods show good concordance in the estimation of ctDNA fraction**

ddPCR is an established methodology to determine ctDNA abundance through direct measurement of tumor-specific somatic mutations in cfDNA. For validation of ichorCNA tumor purity estimates, we assessed the concordance between ddPCR mutation allele fraction (MAF) and ulpWGS ctDNA fraction on 107 baseline and serial samples (73 CSF and 34 plasma). Patient-specific somatic variants, identified from targeted or whole exome sequencing of matched tumor samples (Fig. 3A; Supplementary Table S2), were used to design custom ddPCR assays (Supplementary Table S3 and 4). Figure 3B illustrates findings for two patients in this study. For BCLM+ patient RMH006 (upper panel), ulpWGS estimated a ctDNA fraction of 0.67 and 0.01 in the matched CSF and plasma samples, respectively. ddPCR identified abundant mutant *PIK3CA* E542K copies in primary tumor and CSF, with a mutant CSF allele fraction (MAF) of 0.696, however no plasma *PIK3CA* E542K mutant copies were detected within 746 haploid genome equivalents. In BCLM- patient KCL663 (lower panel), ctDNA was undetectable in both CSF and plasma (ctDNA fraction 0) by ulpWGS. By ddPCR, the *TP53* T253fs variant was found at high MAF (0.596) in the primary tumor, but no mutant *TP53* T253fs copies were detected within 150 and 3300 haploid genome equivalents screened in CSF and plasma, respectively.

There was a strong correlation between ddPCR MAF and ulpWGS ctDNA fraction for the 107 samples undergoing both methods (Fig. 3C, Spearman's  $r = 0.852$ ,  $P < 0.0001$ ; Supplementary Fig. S4A-C showing baseline samples only). The majority of samples 101/107 achieved high-confidence mutation detection at sufficient ddPCR LoD (as defined in Methods), however in the remaining 6 samples (1 baseline CSF; 5 serial CSF) there was insufficient cfDNA yield, attributable to lower sample volumes collected (median 0.55 mL vs. 2.0 mL) (Supplementary Fig. S4D).

### **Assessing the prognostic and predictive potential of monitoring of CSF ctDNA in BCLM**

Of the 24 BCLM+ patients, 19 patients received intrathecal methotrexate and/or trastuzumab therapy, and 6 patients received cranial or spinal radiotherapy (Fig. 4A). In 12 patients undergoing intrathecal therapy, serial CSF samples were collected immediately prior to treatment administration. Baseline ctDNA fraction showed only a weak non-significant correlation with BCLM survival in all 24 BCLM+ patients (Fig. 4B), and there was no significant difference in median overall survival associated with receipt of intrathecal therapy (5.7 months with vs. 3.4 months without intrathecal therapy,  $P = 0.55$ ) (Fig. 4C). Despite this, achieving ctDNA suppression on intrathecal therapy (CSF ctDNA fraction  $< 0.10$ ) was associated with a significantly lengthened survival (Fig. 4D, median survival 11 months vs. 3.25 months,  $P = 0.0337$ ). Furthermore, a reduction in ctDNA fraction from baseline to the second time point (at a median of 3 weeks) was observed more frequently in those achieving PFS  $\geq 6$  months on intrathecal therapy (Fig. 4E).

### **Serial monitoring of CSF ctDNA fraction predicts BCLM relapse on intrathecal therapy**

In the 12 patients undergoing longitudinal sample collection on intrathecal therapy, ctDNA fraction, whether measured by ulpWGS or ddPCR, showed dynamic and quantitative changes on therapy which associated with treatment response, failure to achieve response, and early notification of therapy failure (Fig. 5A-B, Supplementary Fig. S5A-L). CSF cfDNA

concentration and CSF protein levels were not robust indicators of disease status. ddPCR provides two quantitative measures: mutant allele fraction (MAF) and mutant copies per mL of CSF/plasma volume. Both ddPCR measures showed similar trends to ulpWGS in ctDNA fraction monitoring (Supplementary Fig. S5A-L).

Patient KCL553 (Fig. 5A; Supplementary Fig. S5A) commenced intrathecal therapy during week 0 of BCLM diagnosis. The ctDNA fraction of 0.88 by ulpWGS, reduced during treatment to 0.16 at week 15, and was undetectable at week 29, in line with marked improvement in clinical symptoms. MRI at baseline showed decompensated communicating hydrocephalus, which improved on serial imaging at week 28. At week 52, while the patient remained well with stable MRI and negative CSF cytology, the ctDNA fraction rose to 0.27. 12 weeks later the patient developed marked confusion and vomiting, the MRI scan performed showed new abnormal leptomeningeal enhancement, and intrathecal methotrexate was discontinued. The patient succumbed to BCLM 9 weeks later. In patient RMH006 (Fig. 5B; Supplementary Fig. S5B) CSF sample collection started at week 12, at the time of worsened hydrocephalus in the setting of MRI-positive BCLM. At this time point the ctDNA fraction was 0.66 and reduced to undetectable levels during the next 8 weeks of intrathecal methotrexate therapy. At week 18 neurological symptoms were moderately improved, and MRI showed reduction in leptomeningeal enhancement and hydrocephalus. While CSF cytology remained negative, ctDNA fraction rose from the nadir of 0 at week 20, to 0.16 at week 22, and 0.28 at week 28. Malignant cells were later detected on CSF cytology at week 30. MRI imaging at week 25, on retrospective review, showed more conspicuous leptomeningeal enhancement in left internal auditory meatus. Neurological symptoms worsened at week 34 and the patient succumbed to BCLM at week 46. These two cases illustrate the role of ctDNA fraction monitoring for earlier prediction of therapy-failure, which opens up an opportunity window for switching to alternative treatment approaches or, importantly, timely cessation of futile intrathecal therapy and earlier focus on best supportive care.

The other 10 cases (Supplementary Figs S5C-L), provide further examples of the potential clinical utility of ctDNA monitoring. For example, monitoring ctDNA levels could differentiate intracerebral methotrexate toxicity from BCLM progression (Supplementary Figs S5G (KCL625) and S5I (KCL650)) and detect failure of adequate treatment response, as measured by persistently elevated ctDNA fraction, despite apparent improvements in CSF cytology and/or MRI (Supplementary Figs S5F (KCL622), S5H (RMH011) and S5L (5197)).

## Discussion

This proof-of-concept study demonstrates that ulpWGS-assessed CSF ctDNA fraction is a promising tumor-agnostic marker with potential to improve both current diagnostics and therapeutic response monitoring in BCLM. Notably, CSF ctDNA detection correctly identified all BCLM+ cases, while only 50% were detectable through initial CSF cytology. Utilizing ctDNA detection in CSF during diagnostic work-up could therefore avoid the need for multiple lumbar punctures to reach, or confidently refute, BCLM diagnosis.

We demonstrate that both ulpWGS and ddPCR are suitable methods to determine ctDNA fraction in CSF liquid biopsies, with good correlation between approaches. However, ulpWGS is the preferable method since it (a) can be performed without prior primary tumor sequencing, (b) is not constrained by low DNA yields or small volume CSF samples, and (c) provides a more time- and cost-effective approach than ddPCR. Furthermore, the genomic landscape of breast cancer, with relatively few cancer driver mutations but a highly copy number aberrant architecture, is suited to a genome-wide approach for tumor-derived DNA detection (32). Furthermore, ulpWGS was able to detect the acquisition of *ERBB2* amplification, which has an increased occurrence in CNS metastatic disease (33). Although no cases of *ERBB2* amplification occurring in CSF of hitherto HER2-negative cases were found in this study, detection of such events would have clinical use in guiding pharmacotherapeutic options.

This study provides further evidence that CSF is an abundant source of ctDNA in CNS-predominant malignancy, with minimal detection in the plasma unless there was co-existent progression in extracranial metastatic sites. CSF ctDNA fraction in BCLM+ patients (median 0.57, range 0.27 - 0.89), was at much higher abundance than typically found in plasma during progression of systemic metastases (median ~0.05 (34)), in keeping with other reports on CSF ctDNA analysis in primary and metastatic CNS cancer (18,31). Likely explanations for this are the smaller circulating volume of CSF vs. plasma (150 mL (35) vs.

2800 mL (36), respectively), reduced levels of non-tumor, leukocyte-derived cfDNA in CSF (37) and reduced CSF turnover compared to plasma (38). Therefore, although CSF sampling is a more invasive method to obtain liquid biopsy than by simple blood test, there is a clear rationale to sample CSF, which is a rich source of ctDNA for the study of CNS disease.

During the preparation of this manuscript, White *et al.* published findings on a cohort of 22 solid tumor LM patients and, using a similar WGS methodology, demonstrated improved sensitivity and accuracy of ulpWGS-assessed CSF ctDNA for presence of LM when compared to diagnostic cytology (39). This supports the translatability of CSF ctDNA assessment by ulpWGS to other leptomeningeal metastases settings and primary and secondary brain malignancies, where ctDNA is known to be shed into CSF (18,31,40,41).

A major obstacle in treating BCLM is the variability in response to the leptomeningeal-directed therapy of intrathecal chemotherapy. In this study, 10/19 patients receiving intrathecal therapy survived with BCLM for greater than 6 months. However, the invasive nature of this treatment, and difficulty in selecting patients likely to benefit, often discourages its administration. Currently the only response predictors in routine clinical practice during intrathecal therapy are: (a) CSF cytology clearance by 8 weeks (42), and (b) serial MRI imaging, generally assessed 2-3 months following initiation of treatment (12). This study explored the value of early ctDNA monitoring, at a median of 3 weeks into intrathecal therapy. ctDNA suppression (to ctDNA fraction <0.10) during treatment was a significant predictive marker of longer BCLM survival. Conversely, in patients with markedly rising ctDNA fraction at this early time-point, there was a lack of treatment response (failure to achieve PFS >6 months on treatment). Therefore, CSF ctDNA serial monitoring has the potential to identify patients early in treatment for whom invasive intrathecal therapy is unlikely to benefit, thereby allowing a switch to alternative therapeutic approach such as systemic therapy, radiotherapy or novel approaches such as immunotherapy (43). Similarly,

rising ctDNA fraction in patients who initially responded to treatment anticipated BCLM progression by up to 12 weeks. If these findings are validated in an appropriately designed clinical biomarker study, ctDNA measurement in BCLM may allow the option for a timely switch in therapy, prior to patient's performance status declining and precluding further treatments, or an earlier focus on best supportive care.

In conclusion, within the limitations of a small study without pre-defined study design, the data presented provide proof-of-concept for ulpWGS-assessed CSF ctDNA monitoring in BCLM as a potential biomarker to improve current diagnostics and evaluation of treatment response and failure. Prospective assessment in a larger, appropriately designed clinical biomarker validation study (44,45) is warranted, and this should include: an adequate panel of control including patients with brain metastasis without BCLM and patients with non-malignant brain conditions; minimum sample requirements; pre-defined clinical assessments including standardized neurological and radiological evaluations by RANO criteria (12); and establishment of optimal ctDNA diagnostic threshold, to enable a detailed analytical interpretation of the clinical utility of this promising biomarker.

**Author contributions:**

Conception and design: AF, AT, CMI

Sample acquisition: AF, MI, TA, AC, LD, SvL, AO, MH, NT, AT

Sample processing, next-generation sequencing, ddPCR: AF, MI, IGM

Bioinformatic analysis: AM, SH

Neuroradiology review: LC

Data analysis, interpretation: AF, MI, AM, SH, CMI

Writing first draft: AF, MI, AT, CMI

Writing, review, and/or revision of the manuscript: All authors

All authors meet ICMJE criteria and had full access to study data. The corresponding author had final responsibility for the decision to submit for publication.

### **Acknowledgements**

We thank the patients who participated in the studies, along with the study and clinical staff who assisted with the sample collection. For patient enrolment and sample collection in South East London Cancer Research Network, we thank the clinicians S. Irshad, H. Kristeleit, J. Mansi, M. Nathan, E. Sawyer, A. Swampillai and the study nurses and staff R. Liccardo, R. Marlow, and V. Shah for patient enrolment and sample collection. For patient enrolment and sample collection in Royal Marsden NHS Foundation Trust, we thank the clinicians P. Barry, S. Johnston, M. Parton, M Robert and L Ulrich and the study nurses and staff A. Bamba, D. Kelly, S. Thompson. We thank the study nurses and staff in GZA Hospital Sint-Augustinus. We thank M. Beaney and S. Hrieben for laboratory advice and ddPCR assays; J. Seoane and R. Mayor at Vall d'Hebron Institute of Oncology for advice on the extraction of CSF cfDNA, ; the ICR Tumour Profiling Unit and A. Gao for bioinformatics input. This work was supported by: Medical Research Council Clinical Research Training Fellowship (MR/P001564/1; to A Fitzpatrick, C Isacke); NIHR Biomedical Research Centre (BRC) at the Royal Marsden and the ICR post-doctoral support funding (W94500; to A Fitzpatrick); Breast Cancer Now Programme Funding to the Breast Cancer Now Toby Robins Research Centre (CTR-Q4-Y1-5, CTR-Q5-Y1; to C Isacke, N Turner and A Tutt); Breast Cancer Now Research Unit at Kings College London (KCL-Q2-Y1-5, KCL-Q3-Y1; to A Tutt) and Cancer Research UK Centre Grant funding to the Kings College London (CRUK RE15196-9; to A Tutt).

## References

1. Harris M, Howell A, Chrissohou M, Swindell RI, Hudson M, Sellwood RA. A comparison of the metastatic pattern of infiltrating lobular carcinoma and infiltrating duct carcinoma of the breast. *Br J Cancer* 1984;**50**(1):23-30 doi 10.1038/bjc.1984.135.
2. Hyun JW, Jeong IH, Joung A, Cho HJ, Kim SH, Kim HJ. Leptomeningeal metastasis: Clinical experience of 519 cases. *Eur J Cancer* 2016;**56**:107-14 doi 10.1016/j.ejca.2015.12.021.
3. Kingston B, Kayhanian H, Brooks C, Cox N, Chaabouni N, Redana S, *et al.* Treatment and prognosis of leptomeningeal disease secondary to metastatic breast cancer: A single-centre experience. *Breast* 2017;**36**:54-9 doi 10.1016/j.breast.2017.07.015.
4. Morikawa A, Jordan L, Rozner R, Patil S, Boire A, Pentsova E, *et al.* Characteristics and Outcomes of Patients With Breast Cancer With Leptomeningeal Metastasis. *Clin Breast Cancer* 2017;**17**(1):23-8 doi 10.1016/j.clbc.2016.07.002.
5. Straathof CS, de Bruin HG, Dippel DW, Vecht CJ. The diagnostic accuracy of magnetic resonance imaging and cerebrospinal fluid cytology in leptomeningeal metastasis. *J Neurol* 1999;**246**(9):810-4 doi 10.1007/s004150050459.
6. Gauthier H, Guilhaume MN, Bidard FC, Pierga JY, Girre V, Cottu PH, *et al.* Survival of breast cancer patients with meningeal carcinomatosis. *Ann Oncol* 2010;**21**(11):2183-7 doi 10.1093/annonc/mdq232.
7. Glantz MJ, Cole BF, Glantz LK, Cobb J, Mills P, Lekos A, *et al.* Cerebrospinal fluid cytology in patients with cancer: minimizing false-negative results. *Cancer* 1998;**82**(4):733-9 doi 10.1002/(sici)1097-0142(19980215)82:4<733::aid-cncr17>3.0.co;2-z.
8. Le Rhun E, Taillibert S, Zairi F, Kotecki N, Devos P, Mailliez A, *et al.* A retrospective case series of 103 consecutive patients with leptomeningeal metastasis and breast cancer. *J Neurooncol* 2013;**113**(1):83-92 doi 10.1007/s11060-013-1092-8.

9. Wasserstrom WR, Glass JP, Posner JB. Diagnosis and treatment of leptomeningeal metastases from solid tumors: experience with 90 patients. *Cancer* 1982;**49**(4):759-72 doi 10.1002/1097-0142(19820215)49:4<759::aid-cnrcr2820490427>3.0.co;2-7.
10. Clarke JL, Perez HR, Jacks LM, Panageas KS, Deangelis LM. Leptomeningeal metastases in the MRI era. *Neurology* 2010;**74**(18):1449-54 doi 10.1212/WNL.0b013e3181dc1a69.
11. Prommel P, Pilgram-Pastor S, Sitter H, Buhk JH, Strik H. Neoplastic meningitis: How MRI and CSF cytology are influenced by CSF cell count and tumor type. *ScientificWorldJournal* 2013;**2013**:248072 doi 10.1155/2013/248072.
12. Le Rhun E, Devos P, Boulanger T, Smits M, Brandsma D, Ruda R, *et al.* The RANO Leptomeningeal Metastasis Group proposal to assess response to treatment: lack of feasibility and clinical utility and a revised proposal. *Neuro Oncol* 2019;**21**(5):648-58 doi 10.1093/neuonc/noz024.
13. Singh SK, Leeds NE, Ginsberg LE. MR imaging of leptomeningeal metastases: comparison of three sequences. *AJNR Am J Neuroradiol* 2002;**23**(5):817-21.
14. Le Rhun E, Weller M, Brandsma D, Van den Bent M, de Azambuja E, Henriksson R, *et al.* EANO-ESMO Clinical Practice Guidelines for diagnosis, treatment and follow-up of patients with leptomeningeal metastasis from solid tumours. *Ann Oncol* 2017;**28**(suppl\_4):iv84-iv99 doi 10.1093/annonc/mdx221.
15. Boogerd W, van den Bent MJ, Koehler PJ, Heimans JJ, van der Sande JJ, Aaronson NK, *et al.* The relevance of intraventricular chemotherapy for leptomeningeal metastasis in breast cancer: a randomised study. *Eur J Cancer* 2004;**40**(18):2726-33 doi 10.1016/j.ejca.2004.08.012.
16. Bonneau C, Paintaud G, Tredan O, Dubot C, Desvignes C, Dieras V, *et al.* Phase I feasibility study for intrathecal administration of trastuzumab in patients with HER2 positive breast carcinomatous meningitis. *Eur J Cancer* 2018;**95**:75-84 doi 10.1016/j.ejca.2018.02.032.

17. Raizer J, Pentsova E, Omuro A, Lin N, Nayak L, Quant E, *et al.* Phase I Trial of Intrathecal Trastuzumab in Her2 Positive Leptomeningeal Metastases. *Neuro-Oncology* 2014;**16** doi 10.1093/neuonc/nou237.46.
18. De Mattos-Arruda L, Mayor R, Ng CKY, Weigelt B, Martinez-Ricarte F, Torrejon D, *et al.* Cerebrospinal fluid-derived circulating tumour DNA better represents the genomic alterations of brain tumours than plasma. *Nat Commun* 2015;**6**:8839 doi 10.1038/ncomms9839.
19. Momtaz P, Pentsova E, Abdel-Wahab O, Diamond E, Hyman D, Merghoub T, *et al.* Quantification of tumor-derived cell free DNA(cfDNA) by digital PCR (DigPCR) in cerebrospinal fluid of patients with BRAFV600 mutated malignancies. *Oncotarget* 2016;**7**(51):85430-6 doi 10.18632/oncotarget.13397.
20. Huang R, Xu X, Li D, Chen K, Zhan Q, Ge M, *et al.* Digital PCR-Based Detection of EGFR Mutations in Paired Plasma and CSF Samples of Lung Adenocarcinoma Patients with Central Nervous System Metastases. *Target Oncol* 2019;**14**(3):343-50 doi 10.1007/s11523-019-00645-5.
21. Sasaki S, Yoshioka Y, Ko R, Katsura Y, Namba Y, Shukuya T, *et al.* Diagnostic significance of cerebrospinal fluid EGFR mutation analysis for leptomeningeal metastasis in non-small-cell lung cancer patients harboring an active EGFR mutation following gefitinib therapy failure. *Respir Investig* 2016;**54**(1):14-9 doi 10.1016/j.resinv.2015.07.001.
22. Shingyoji M, Kageyama H, Sakaida T, Nakajima T, Matsui Y, Itakura M, *et al.* Detection of epithelial growth factor receptor mutations in cerebrospinal fluid from patients with lung adenocarcinoma suspected of neoplastic meningitis. *J Thorac Oncol* 2011;**6**(7):1215-20 doi 10.1097/JTO.0b013e318219aaae.
23. Garcia-Murillas I, Schiavon G, Weigelt B, Ng C, Hrebien S, Cutts RJ, *et al.* Mutation tracking in circulating tumor DNA predicts relapse in early breast cancer. *Sci Transl Med* 2015;**7**(302):302ra133 doi 10.1126/scitranslmed.aab0021.

24. Adalsteinsson VA, Ha G, Freeman SS, Choudhury AD, Stover DG, Parsons HA, *et al.* Scalable whole-exome sequencing of cell-free DNA reveals high concordance with metastatic tumors. *Nat Commun* 2017;**8**(1):1324 doi 10.1038/s41467-017-00965-y.
25. Cibulskis K, Lawrence MS, Carter SL, Sivachenko A, Jaffe D, Sougnez C, *et al.* Sensitive detection of somatic point mutations in impure and heterogeneous cancer samples. *Nat Biotechnol* 2013;**31**(3):213-9 doi 10.1038/nbt.2514.
26. Wang K, Li M, Hakonarson H. ANNOVAR: functional annotation of genetic variants from high-throughput sequencing data. *Nucleic Acids Res* 2010;**38**(16):e164 doi 10.1093/nar/gkq603.
27. Pascual J, Lim JSJ, Macpherson IR, Armstrong AC, Ring A, Okines AFC, *et al.* Triplet Therapy with Palbociclib, Taselisib, and Fulvestrant in PIK3CA-Mutant Breast Cancer and Doublet Palbociclib and Taselisib in Pathway-Mutant Solid Cancers. *Cancer Discov* 2021;**11**(1):92-107 doi 10.1158/2159-8290.CD-20-0553.
28. Sondka Z, Bamford S, Cole CG, Ward SA, Dunham I, Forbes SA. The COSMIC Cancer Gene Census: describing genetic dysfunction across all human cancers. *Nat Rev Cancer* 2018;**18**(11):696-705 doi 10.1038/s41568-018-0060-1.
29. Niwinska A, Rudnicka H, Murawska M. Breast cancer leptomeningeal metastasis: propensity of breast cancer subtypes for leptomeninges and the analysis of factors influencing survival. *Med Oncol* 2013;**30**(1):408 doi 10.1007/s12032-012-0408-4.
30. Angus L, Deger T, Jager A, Martens JWM, de Weerd V, van Heuvel I, *et al.* Detection of Aneuploidy in Cerebrospinal Fluid from Patients with Breast Cancer Can Improve Diagnosis of Leptomeningeal Metastases. *Clin Cancer Res* 2021;**27**(10):2798-806 doi 10.1158/1078-0432.CCR-20-3954.
31. Pentsova EI, Shah RH, Tang J, Boire A, You D, Briggs S, *et al.* Evaluating Cancer of the Central Nervous System Through Next-Generation Sequencing of Cerebrospinal Fluid. *J Clin Oncol* 2016;**34**(20):2404-15 doi 10.1200/JCO.2016.66.6487.

32. Cancer Genome Atlas N. Comprehensive molecular portraits of human breast tumours. *Nature* 2012;**490**(7418):61-70 doi 10.1038/nature11412.
33. Priedigkeit N, Hartmaier RJ, Chen Y, Vareslija D, Basudan A, Watters RJ, *et al.* Intrinsic Subtype Switching and Acquired ERBB2/HER2 Amplifications and Mutations in Breast Cancer Brain Metastases. *JAMA Oncol* 2017;**3**(5):666-71 doi 10.1001/jamaoncol.2016.5630.
34. Rossi G, Mu Z, Rademaker AW, Austin LK, Strickland KS, Costa RLB, *et al.* Cell-Free DNA and Circulating Tumor Cells: Comprehensive Liquid Biopsy Analysis in Advanced Breast Cancer. *Clin Cancer Res* 2018;**24**(3):560-8 doi 10.1158/1078-0432.CCR-17-2092.
35. Sakka L, Coll G, Chazal J. Anatomy and physiology of cerebrospinal fluid. *Eur Ann Otorhinolaryngol Head Neck Dis* 2011;**128**(6):309-16 doi 10.1016/j.anorl.2011.03.002.
36. Yiengst MJ, Shock NW. Blood and plasma volume in adult males. *J Appl Physiol* 1962;**17**:195-8 doi 10.1152/jappl.1962.17.2.195.
37. Snyder MW, Kircher M, Hill AJ, Daza RM, Shendure J. Cell-free DNA Comprises an In Vivo Nucleosome Footprint that Informs Its Tissues-Of-Origin. *Cell* 2016;**164**(1-2):57-68 doi 10.1016/j.cell.2015.11.050.
38. Pardridge WM. CSF, blood-brain barrier, and brain drug delivery. *Expert Opin Drug Deliv* 2016;**13**(7):963-75 doi 10.1517/17425247.2016.1171315.
39. White MD, Klein RH, Shaw B, Kim A, Subramanian M, Mora JL, *et al.* Detection of Leptomeningeal Disease Using Cell-Free DNA From Cerebrospinal Fluid. *JAMA Network Open* 2021;**4**(8):e2120040-e doi 10.1001/jamanetworkopen.2021.20040.
40. Mouliere F, Mair R, Chandrananda D, Marass F, Smith CG, Su J, *et al.* Detection of cell-free DNA fragmentation and copy number alterations in cerebrospinal fluid from glioma patients. *EMBO Mol Med* 2018;**10**(12) doi 10.15252/emmm.201809323.

41. Pan W, Gu W, Nagpal S, Gephart MH, Quake SR. Brain tumor mutations detected in cerebral spinal fluid. *Clin Chem* 2015;**61**(3):514-22 doi 10.1373/clinchem.2014.235457.
42. Clatot F, Philippin-Lauridant G, Ouvrier MJ, Nakry T, Laberge-Le-Couteulx S, Guillemet C, *et al.* Clinical improvement and survival in breast cancer leptomeningeal metastasis correlate with the cytologic response to intrathecal chemotherapy. *J Neurooncol* 2009;**95**(3):421-6 doi 10.1007/s11060-009-9940-2.
43. Brastianos PK, Lee EQ, Cohen JV, Tolaney SM, Lin NU, Wang N, *et al.* Single-arm, open-label phase 2 trial of pembrolizumab in patients with leptomeningeal carcinomatosis. *Nat Med* 2020;**26**(8):1280-4 doi 10.1038/s41591-020-0918-0.
44. Hayes DF. Defining Clinical Utility of Tumor Biomarker Tests: A Clinician's Viewpoint. *J Clin Oncol* 2021;**39**(3):238-48 doi 10.1200/JCO.20.01572.
45. Hayes DF. Biomarker validation and testing. *Mol Oncol* 2015;**9**(5):960-6 doi 10.1016/j.molonc.2014.10.004.

<b>Table 1. Clinical data (n=30)</b>						
<b>Study ID</b>	<b>Diagnostic group</b>	<b>Primary tumor histological subtype</b>	<b>Neuroaxis MRI*</b>	<b>CSF sampling procedures (n)</b>	<b>CSF cytology - initial/final</b>	<b>CSF collection site</b>
KCL449	BCLM +	HR+ HER2-, ILC	Pos	2	Neg/Pos	Ventricular (Om)
KCL448	BCLM +	HR+ HER2-, IDC/ILC	Pos	1	Pos	Lumbar
KCL523	BCLM +	HR+ HER2-, IDC/ILC	Pos	1	Pos	Lumbar
KCL450	BCLM +	HR+ HER2-, ILC	Pos	1	Pos	Lumbar
KCL499	BCLM +	TN, IDC	Pos	1	Susp	Lumbar
KCL553	BCLM +	HR+ HER2-, ILC	Borderline	2	Neg/Pos	Lumbar
KCL566	BCLM +	HR+ HER2-, IDC	Borderline	1	Pos	Lumbar
RMH006	BCLM +	HR+ HER2-, IDC	Pos	1	Susp	Ventricular (VP)
KCL590	BCLM +	HR+ HER2-, IDC	Pos	2	Neg/Susp	Lumbar
KCL148	BCLM +	HR+ HER2-, ILC	Pos	1	Pos	Lumbar
KCL320	BCLM +	HR+ HER2-, ILC	Borderline	2	Neg/Pos	Lumbar
RMH008	BCLM +	HR+ HER2+, IDC/ILC	Pos	1	Pos	Lumbar
KCL610	BCLM +	HR+ HER2-, ILC	Pos	1	Pos	Lumbar
KCL616	BCLM +	HR+ HER2-, ILC	NP	2	Neg/Susp	Lumbar
KCL617	BCLM +	HR- HER2+, IDC	Pos	1	Neg	Lumbar
KCL622	BCLM +	TN, ILC	Pos	1	Pos	Ventricular (Om)
KCL625	BCLM +	TN, IDC	Borderline	2	Neg/Pos	Ventricular (Om)
RMH010	BCLM +	HR+ HER2-, ILC	Pos	1	Pos	Lumbar
RMH011	BCLM +	HR+ HER2+, IDC	Pos	5	Neg/Neg	Lumbar
KCL650	BCLM +	TN, IDC	Pos	1	Pos	Lumbar
KCL658	BCLM +	TN, IDC	Pos	1	Pos	Lumbar
KCL680	BCLM +	HR+ HER2-, ILC	Pos	2	Neg/Neg	Lumbar
5197	BCLM +	HR+ HER2-, ILC	Pos	1	Pos	Ventricular (Om)
5225	BCLM +	HR+ HER2-, IDC	Pos	1	Neg	Lumbar
RMH002	BCLM -	HR- HER2+, IDC	Neg	1	Neg	Lumbar
RMH004	BCLM -	HR- HER2+, IDC	Neg	1	Neg	Lumbar
RMH007	BCLM -	HR- HER2+, IDC	Neg	1	Neg	Lumbar
RMH005	BCLM -	HR- HER2+, IDC	Neg	1	Neg	Lumbar
RMH009	BCLM -	HR+ HER2-, IDC	Neg	1	Neg	Lumbar
KCL663	BCLM -	TN, NST	Neg	2	Neg/Neg	Lumbar

**General abbreviations;** BCLM, breast cancer leptomeningeal metastasis; HER2, human epidermal growth factor receptor 2; HR, hormone receptor; IDC, invasive ductal carcinoma; ILC, invasive lobular carcinoma; MRI, magnetic resonance imaging; NP, not performed; Neg, negative; NST, no special type; Om, Ommaya; Pos, positive; Susp, suspicious; TN, triple negative; VP, ventriculoperitoneal shunt.

\*Neuroaxis MRI results following independent neurological review.

## Figure Legends

**Figure 1.** CSF and plasma cfDNA extraction and tumor fraction estimation by ultra-low pass whole genome sequencing (ulpWGS). (A) Schematic showing baseline and serial sample collection for the study. (B) CSF cfDNA concentration (ng/mL) in paired baseline CSF and plasma samples ( $n=28$ ). Violin plots show median and IQR (paired  $t$ -test on log-transformed values.) (C) Schematic showing pipeline for cfDNA ulpWGS and assessment of tumor fraction. (D) Representative cfDNA ulpWGS genome-wide copy number plots ( $\log_2$  ratio) for paired CSF and plasma samples. Fraction of circulating tumor DNA in cfDNA (ctDNA fraction) purity estimates by ichorCNA are shown for cases KCL449 (BCLM+), KCL650 (BCLM+) and RMH009 (BCLM-).

## Figure 2.

ulpWGS measurement of CSF ctDNA fraction in the diagnosis of BCLM. (A) ctDNA fraction in baseline CSF samples from patients with a suspected diagnosis of BCLM who subsequently had a confirmed diagnosis (BCLM+;  $n=24$ ) or did not develop leptomeningeal disease on follow-up (BCLM-;  $n=6$ ). Symbol color indicates CSF cytology result on initial LP (Mann-Whitney  $U$ -test). (B) CSF ctDNA fraction in BCLM+ samples according to MRI imaging for BCLM (unpaired  $t$ -test). (C) CSF ctDNA fraction in BCLM- patients who had or had not a subsequent diagnosis of breast cancer brain metastasis (BCBM) (unpaired  $t$ -test) (D) Correlation of CSF ctDNA fraction and CSF cfDNA concentration. Symbol color denotes the BCLM diagnostic status (Pearson's  $r$  correlation). (E) ctDNA fraction in paired baseline CSF and plasma samples from BCLM+ ( $n=22$  pairs) and BCLM- ( $n=5$  pairs) patients (unpaired  $t$ -tests). (F) Plasma ctDNA fraction in BCLM+ patients with no evidence of extracranial progressive disease (PD), as assessed by imaging, within 3 months of BCLM diagnosis (No PD;  $n=17$  vs. those with evidence of extracranial PD;  $n=8$ ; unpaired  $t$ -test). Symbol color indicates patients who previously received whole brain radiotherapy (WBRT).

KCL499 and RMH008 (both no PD) received WBRT for parenchymal brain metastasis at 1.1 and 15.8 months prior to BCLM diagnosis.

**Figure 3.** Comparison of ulpWGS and ddPCR methods of ctDNA content assessment. (A) Schematic showing the pipeline for ddPCR-based ctDNA fraction assessment. Genomic DNA (gDNA) was extracted from archival tumor and subject to targeted or whole exome sequencing to identify high confidence somatic variants for the design of custom droplet digital PCR (ddPCR) assays. (B) Representative examples. Upper panels: genome-wide copy number variation plots of primary tumor determined by whole-exome sequencing (WES) and paired CSF and plasma cfDNA samples determined by ulpWGS with ctDNA fraction purity estimates by ichorCNA. Lower panels: ddPCR plots for *PIK3CA* p.E542K (RMH006) or *TP53* p.T253fs (KCL663) variants (FAM-positive droplets indicated within the marked area) or wild type *PIK3CA/TP53* (VIC-positive droplets) in the primary tumor, CSF and plasma with mutant allele fraction (MAF) indicated. (C) Correlation of ctDNA fraction (ulpWGS) and ddPCR mutant allele fraction (MAF) in the 107 CSF and plasma samples (baseline and serial) which underwent both methods (Spearman's rank correlation). Legend colors indicate samples which passed or failed ddPCR LoD (as defined in Methods). Left plot provides an expanded view of the samples with ddPCR MAF and/or ctDNA fraction <0.15.

**Figure 4.** BCLM treatment and longitudinal monitoring of CSF ctDNA fraction. (A) Swimmer plot of BCLM+ patients with type/duration of intrathecal therapy, date of whole brain or spinal radiotherapy (RT) completion when administered, and timepoints and route of CSF collection indicated. Ventricular samples were collected via Ommaya reservoir except RMH006 who had a ventriculoperitoneal shunt. Note 5/24 patients did not receive intrathecal therapy. (B) Correlation of baseline CSF ctDNA fraction vs. BCLM overall survival (months from BCLM diagnosis) for all BCLM+ cases (Spearman's rank correlation). (C) Kaplan-Meier overall survival curves of all BCLM+ cases by intrathecal therapy received ( $n=19$ ) or not

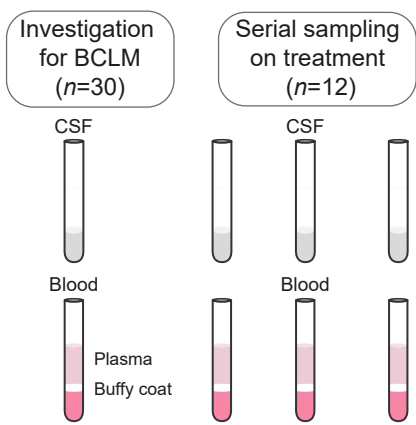
received ( $n=5$ ), with survival in months from BCLM diagnosis. (D) Kaplan-Meier overall survival curves in 12 patients who underwent serial ctDNA monitoring on intrathecal therapy, comparing survival when ctDNA fraction of  $<0.10$  was achieved ( $n=7$ ), versus those where ctDNA remained  $\geq 0.10$  ( $n=5$ ). Survival shown in months from start of intrathecal therapy. (E) Waterfall plot showing change in ctDNA between baseline and second serial timepoint (median 3 weeks from baseline ctDNA measurement). BCLM responders were defined as those with progression free survival (PFS) of  $\geq 6$  months, or patients who showed clinical response to intrathecal therapy but had extracranial disease progression leading to cessation of intrathecal therapy.

**Figure 5.** CSF ctDNA fraction tracks with clinical responses and predicts relapse on intrathecal therapy. Examples of longitudinal monitoring of BCLM+ patients (A) KCL553 and (B) RMH006 receiving intrathecal therapy. Shown are: CSF ctDNA fraction assessed by ulpWGS; CSF ddPCR mutant copies/mL for variant *HIF1A* p.A565G (KCL553) and *PIK3CA* p.E542K (RMH006); CSF cytology, (“-“ = no malignant/abnormal cells, “+” = malignant or suspicious atypical cells identified; Clinical symptoms A = absence of neurological symptoms, M = mild neurological symptoms, S = severe neurological symptoms. Shaded blocks indicate intrathecal chemotherapy (methotrexate; yellow, methotrexate + trastuzumab; blue). x axis ends at week of patients’ death; MRI, Dx = diagnosis, PR = partial response, SD = stable disease, PD = progressive disease. MRI images shown as follows (5A, left) T2-weighted FLAIR sequence showing decompensated communicating hydrocephalus depicted by lateral ventriculomegaly (yellow arrowhead) and peri-ependymal oedema (red arrowhead); (5A, middle) T2-weighted FLAIR sequence showing reduction in hydrocephalus since the prior study (yellow arrow); (5A, right) T1-weighted contrast-enhanced sequence demonstrating leptomeningeal enhancement within the internal auditory meati bilaterally (red arrowheads), more pronounced on the patient’s left; (5B, left) T1-weighted contrast-enhanced sequence showing leptomeningeal enhancement within the cerebellar sulci (red arrowhead). (5B, middle) T2-weighted FLAIR sequence showing new

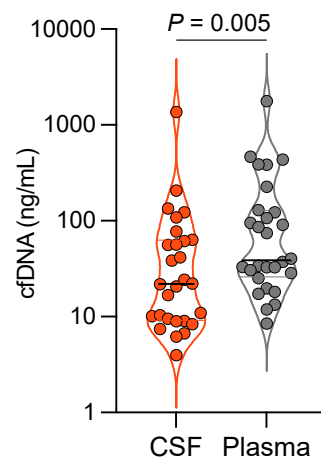
communicating hydrocephalus (yellow arrowhead) and early peri-ependymal oedema (red arrowhead); (5B, right) T1-weighted contrast-enhanced sequence showing leptomeningeal enhancement within the left internal auditory meatus (red arrowhead).

# Figure 1

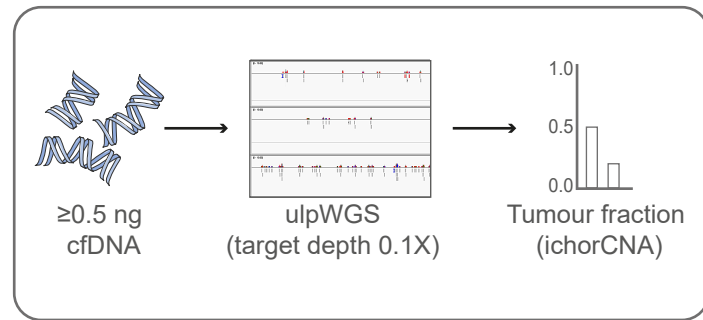
A



B



C



D

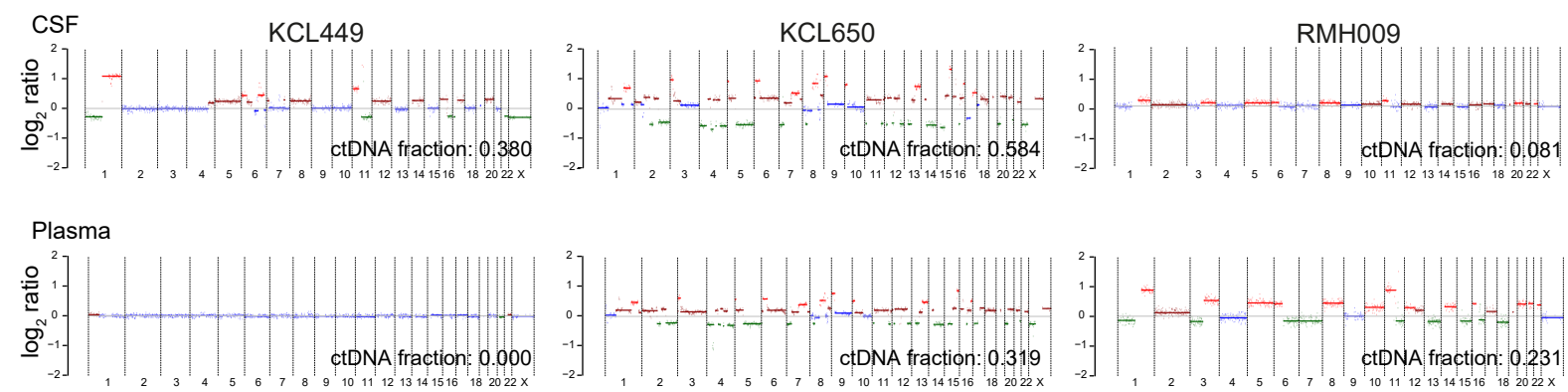


# Figure 2

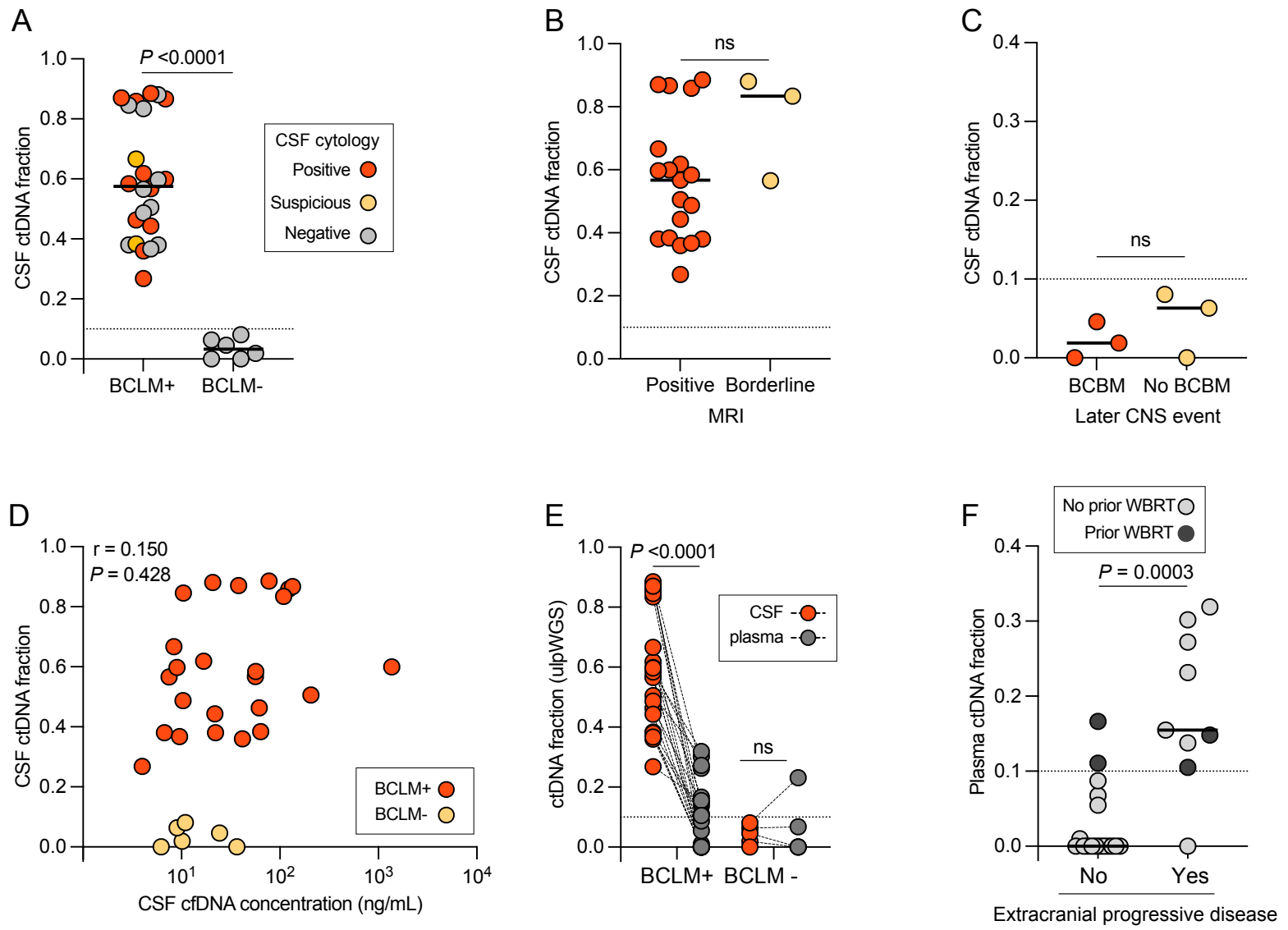
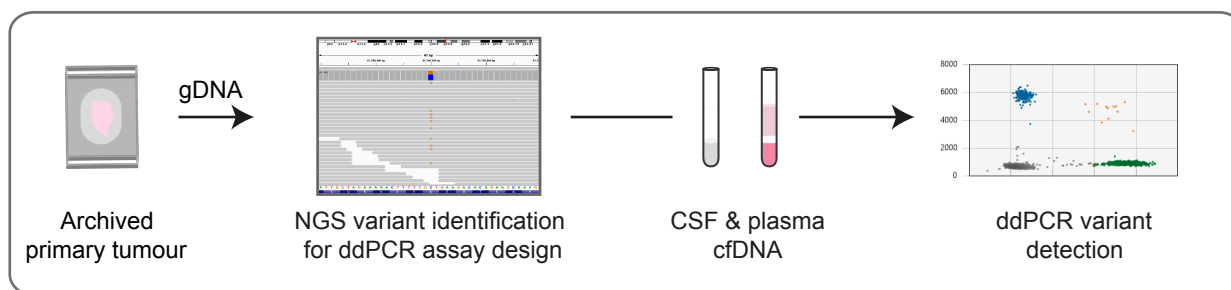
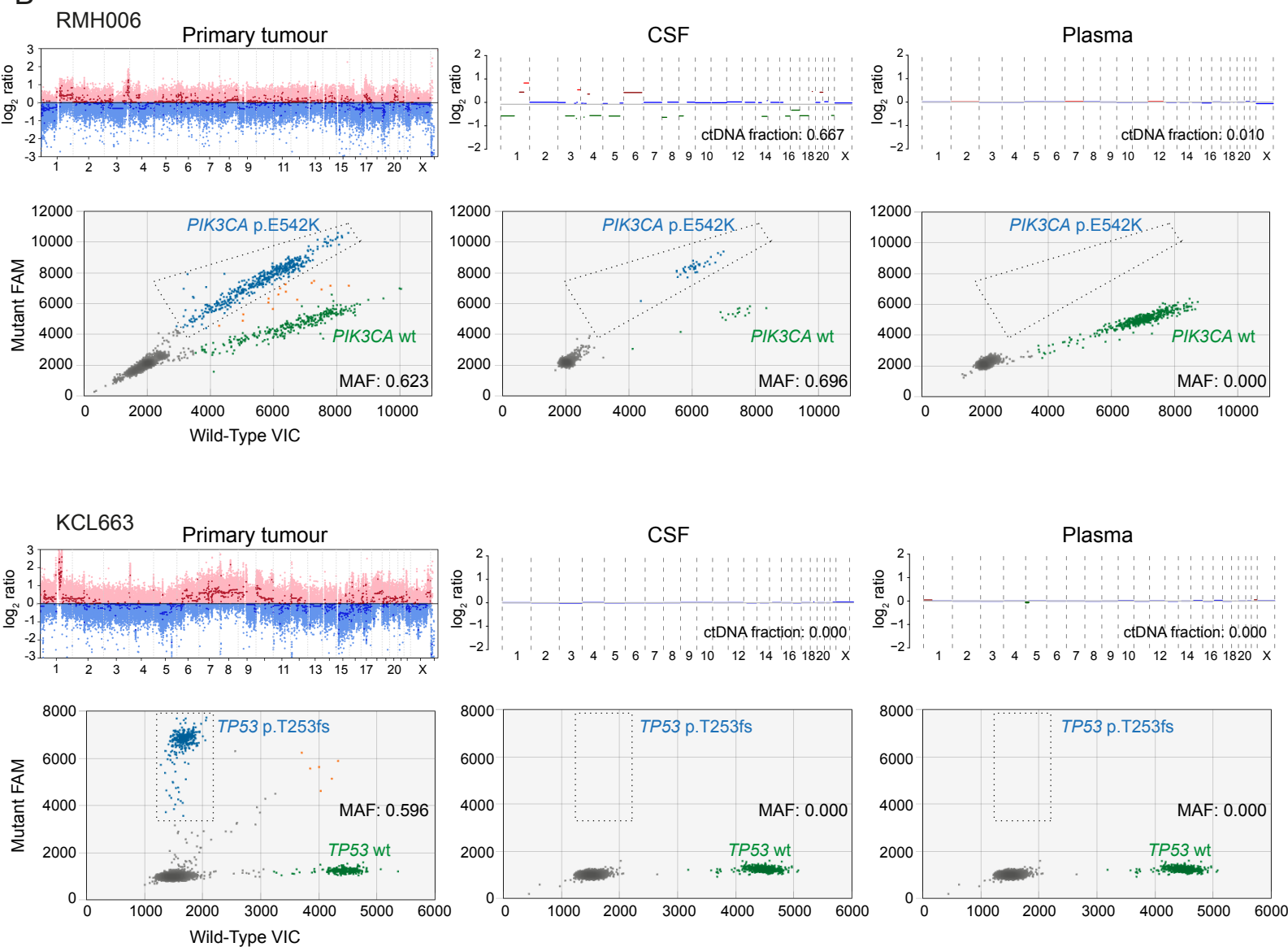


# Figure 3

A



B



C

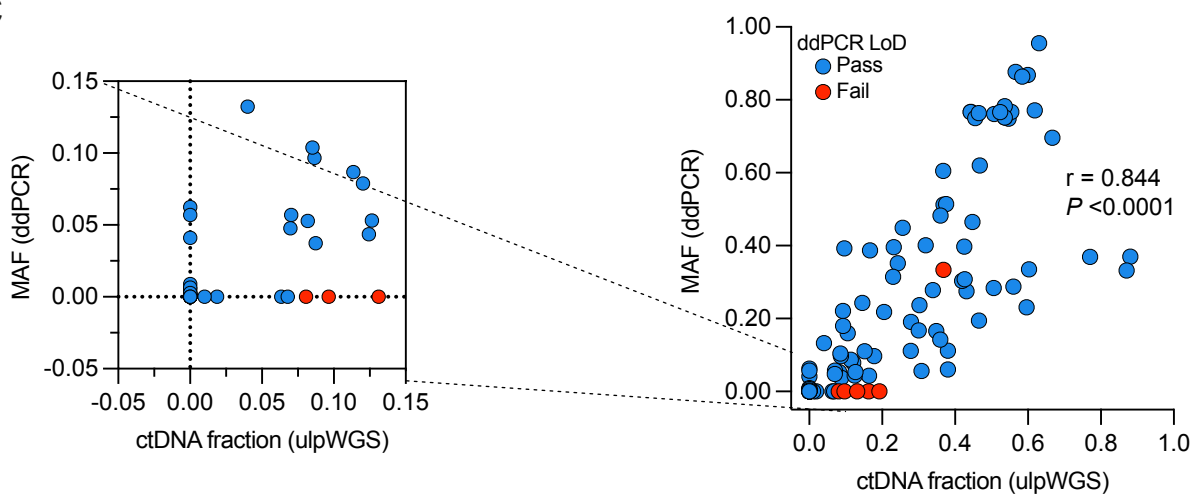
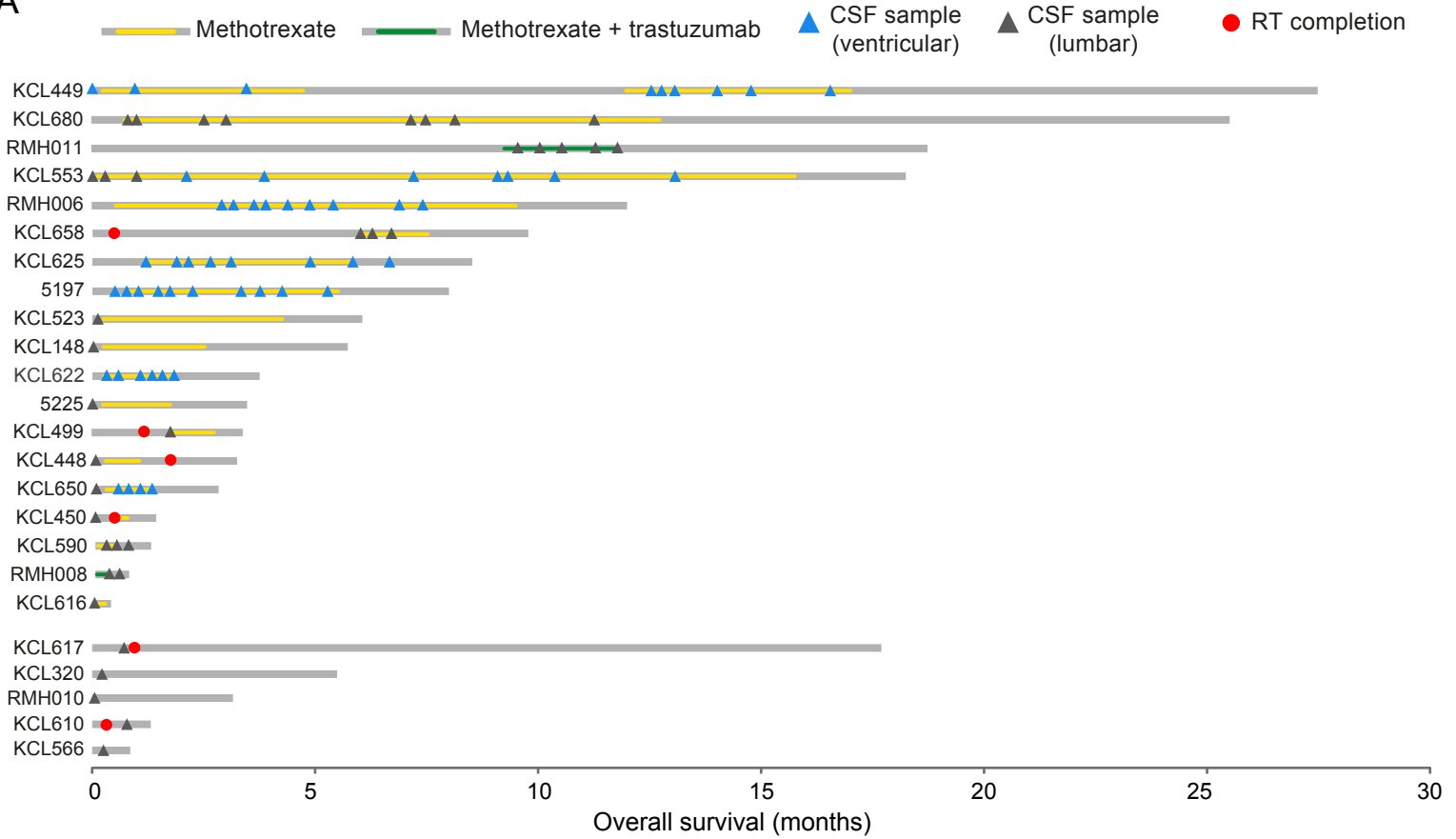
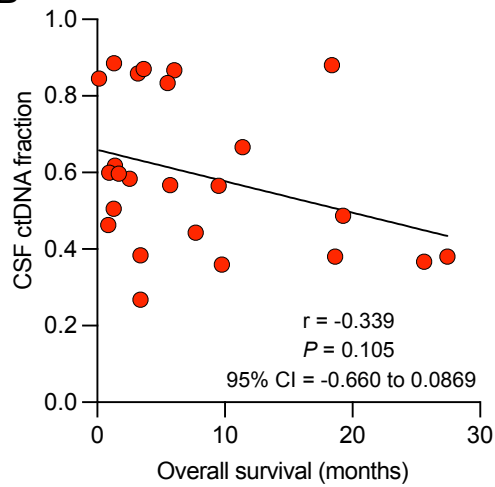


# Figure 4

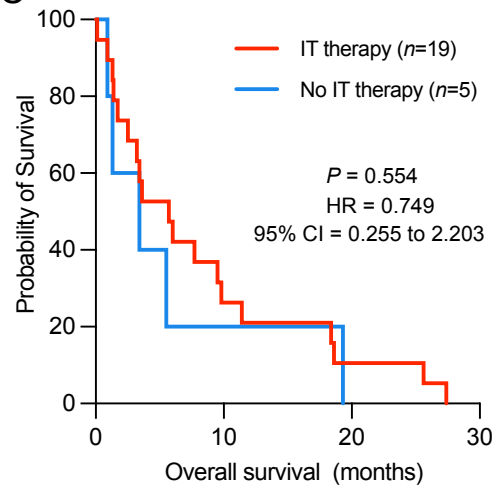
## A



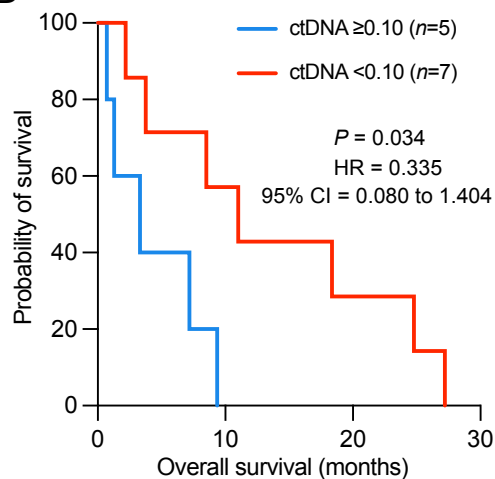
## B



## C



## D



## E

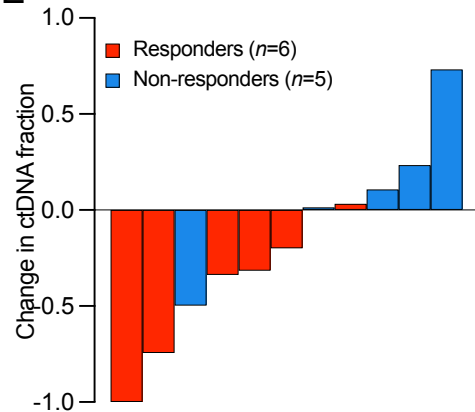


# Figure 5

